The aid of calorimetry for kinetic and thermal study

Balsam Belgacem, Sébastien Leveneur, Mohamed Chlendi, Lionel Estel, Mohamed Bagane

THE AID OF CALORIMETRY FOR KINETIC AND THERMAL STUDY: APPLICATION TO THE DISSOLUTION OF TUNISIAN NATURAL PHOSPHATES

Balsam Belgacem[1], Sébastien Leveneur[2,3], Mohamed Chlendi[1], Lionel Estel[2], Mohamed Bagane[1]

1. Chemical Engineering Department, National Engineering School of Gabes (ENIG) University of Gabes, Tunisia

2. LSPC-Laboratoire de Sécurité des Procédés Chimiques, INSA Rouen, BP08, Avenue de l'Université, 76801 Saint-Etienne-du-Rouvray, France; E-mail : sebastien.leveneur@insa-rouen.fr; fax: +33 2 32 95 66 52.

3. Laboratory of Industrial Chemistry and Reaction Engineering, Process Chemistry Centre, Åbo Akademi University, Biskopsgatan 8, FI-20500 Åbo/Turku, Finland.

Abstract

Phosphoric acid, non-renewable chemical, is used in different industries. Production of this chemical from natural phosphate can be done by two routes: wet-process and thermal-process. The nature of the natural phosphate, i.e., its chemical composition, plays an important role on the kinetics and thermodynamics of phosphoric acid production. Thus, the establishment of a kinetic model, based on reaction mechanism, for the dissolution of natural phosphate is cumbersome due to the presence of impurities. Besides, one should use an online analytical method because the dissolution reaction is fast.

The dissolution of two natural phosphates with different percentage of phosphorus pentoxide (P_2O_5), phosphate samples (28 wt. % of P_2O_5) from Gafsa region (Tunisia) and phosphate samples (18 wt.% of P_2O_5) from Cheketma-Kasserine region (Tunisia), were studied from a kinetic and thermal aspects. Experiments were performed by using a Tian-Calvet calorimeter. Two acid solutions were used for the dissolution, one with phosphoric acid (S1) and the other a mixture of phosphoric and sulfuric acid (S2).

For both natural phosphate, it was found that in case of using S1 solution the heat released due to the dissolution was lower than in case of using solution S2. This difference was explained by the precipitation of monohydrate sulfate calcium to its dihydrate form. By using a granulometry distribution lower than 500 µm, heat released during the dissolution of both phosphates by S1 was similar, i.e., -230 J g^{-1}, and the same observation was done by using S2 solution, i.e., between -300 and -350 J g^{-1}. We have demonstrated that granulometry distribution plays an important role, and by using a granulometry lower than 120 µm for Cheketma-Kasserine region phosphate, the heat released during the dissolution was higher, i.e., -400 J g^{-1} with solution S2. Avrami model was found to describe the precipitation of calcium sulfate, and three distinguished domains were obtained by using Gafsa region phosphate compared to two domains with Cheketma-Kasserine region phosphate.

Keywords: Tian-Calvet calorimeter, natural phosphate, dissolution, thermodynamics, kinetics, Avrami equation.

1. Introduction

Phosphorus compounds are essential in the production of agricultural fertilizers and for chemical products such as phosphoric acid [1-2]. The raw material for these compounds are non-renewable natural phosphate rocks. Phosphate, which is a phosphorus pentoxide P_2O_5, is a general term that describes natural mineral aggregations containing a high phosphoric mineral concentration [3]. In general, phosphate is associated with oxygen to form phosphate radicals PO_4^{3-} which can combine with more than 30 elements [4]. The most common phosphate minerals are apatites, and mainly fluorapatite, $Ca_5(PO_4)_3F$.

Phosphoric acid can be produced by wet process. According to the operating conditions, one can distinguish:

- Wet hemihydrate process: formation of hemihydrate precipitate (HH) $CaSO_4.1/2H_2O$,
- Wet dihydrate process: formation of dihydrate precipitate (DH) $CaSO_4.2H_2O$, also known as gypsum,

Phosphoric acid production in Tunisia is carried out by the wet dihydrate process. The manufacturing is made by the attack in humid environment of crushed phosphate, treated and enriched by diluted phosphoric acid and concentrated sulfuric acid solution. The choice of these acids results from the formation of insoluble calcium sulfate precipitation, which is afterward separated from phosphoric acid by filtration. On the other hand, attack by nitric or hydrochloric acid leads to a soluble precipitation of calcium chloride or nitrate which can make the separation difficult or economically unfeasible [4].

Dissolution of phosphate in mixed acid solution (phosphoric and sulfuric acids) is conducted in two steps [5]. In a first step, the phosphoric acid attacks the particles of the phosphate ores to form the soluble mono-calcium phosphate:

$$2Ca_5(PO_4)_3F + 14H_3PO_4 \rightarrow 10Ca(H_2PO_4)_2 + 2HF \quad (1)$$

In a second step, the mono-calcium phosphate reacts with sulfuric acid to form a calcium sulfate precipitate.

$$Ca(H_2PO_4)_2 + H_2SO_4 + 2H_2O \rightarrow 2H_3PO_4 + CaSO_4.2H_2O \quad (2)$$

The kinetics of such dissolution can be cumbersome. For that reason, several authors used the Avrami model to describe the dissolution mechanism. For instance, dissolution of synthesized fluorapatite ($Ca_5(PO_4)_3F$) in a mixture phosphoric and sulfuric acid solution was studied by Antar et al. [6]. The Avrami model showed a curve with two fields demonstrating that the attack was done in two steps. The first domain corresponds to the dissolution of the fluorapatite by phosphoric acid. The second field is linked to the formation of the dehydrate precipitate by sulfuric acid according to the following reaction:

$$Ca(H_2PO_4)^+ + H^+ + 2H_2O \rightarrow CaSO_4.2H_2O + H_3PO_4 \quad (3)$$

Brahim et al. [7] showed that the dissolution of the synthesized fluorapatite in phosphoric acid solution is made in two steps of dissolution mechanism, which were confirmed by the experimental results and calculation.

The natural rock phosphate attacked by acid is more complex than in the case of synthesized fluorapatite. Some kinetic and thermodynamic studies have proposed some mechanisms for the phosphate rock digestion in phosphoric acid or in sulfuric acid [8-9]. Further works were devoted by the study of dissolution of natural fluorapatite in a mixture of these acids [10]. Because of the multiple components in natural rocks, it is impossible to derive a kinetic model based on reaction mechanism obtained from calorimeter data. The application of the Avrami model shows the succession of steps leading eventually to the gypsum precipitation $CaSO_4.2H_2O$ as Antar and Jemal [10] showed it with the dissolution of fluorapatite.

The literature survey reveals the presence of other works including thermodynamic and kinetic studies of phosphate attack by acids. For example, Vaimakis et al. [11] studied the reaction mechanism of selective dissolution of calcite found in phosphate ores by diluted acetic acid, and Soussi-Baatout et al. [12] studied the thermodynamics of the phosphate attack by hydrochloric acid.

The present work aims to study the thermodynamics and the kinetics of the dissolution of natural phosphate rocks with two different concentrations of P_2O_5. The influence of the particle size was also studied, which was not found in the literature.

2. Experimental section

2.1. Experimental apparatus and function

A Tian-Calvet calorimeter (C80, SETARAM) shown in Fig. 1, was used to study the thermodynamics and the kinetics of the phosphate attack by acid solutions.

To perform these experiments, reversal mode with a measuring and a reference cell was used. They contain two compartments separated by a lid. The mass of solid phosphate reactant was introduced in the lower compartment. The acid solution was introduced into the upper compartment as shown in Fig. 1. More information about the use of this calorimeter can be found in articles of our group [13-14].

When the cells were filled with reactants and solution, they were placed in the calorimetric block. When the desired temperature was reached and heat flow rate was stable, the calorimeter was put on reversal mode.

According to the C80 manufacturer, the accuracies of enthalpy and temperature are 0.1% and 0.1 °C, respectively.

Here Fig. 1

2.2 Chemicals

The phosphate rocks were supplied by the "*Groupe Chimique Tunisien (GCT)*". The first type of rocks is phosphate from Gafsa (28.89% P_2O_5), enriched by the GCT and the second type of rocks is phosphate from Cheketma-Kasserine (18.42% P_2O_5).

Three samples of phosphate with different granulometry were used:

-Sample PG1 was the phosphate from Gafsa with a granulometry G1 (lower than 500µm),

-Sample PK1 was the low phosphate from Cheketma-Kasserine with a granulometry G2 (lower than 500µm),

-Sample PK2 was of the same low phosphate from Cheketma-Kasserine having a granulometry G3 (lower than 120µm). It was obtained by crushing PK1 in a mortar.

Different acid solutions were tested:

-Solution S1 is a phosphoric acid solution having 20 mass/% of P_2O_5.

-Solution S2 is a mixture of 80 volume/% of S1 and 20 volume/% of a sulfuric acid at a weight percent of 90%.

Different masses of solid phosphate were used from 19.99 mg to 303.88 mg and keeping the same volume 4.65 mL of acid solution.

3. Results and discussion

3.1. Dissolution of the enriched phosphate of Gafsa (PG1) at 25°C

Dissolution of the phosphate of Gafsa PG1 was carried out in the phosphoric acid solution S1 with various masses. Fig. 2 shows the evolution of heat flow rate of dissolution versus the initial mass of Gafsa phosphate. One can notice that dissolution of phosphate is an exothermic reaction.

Here Fig. 2

The heat flow rate increases when the amount of phosphate increases. The results of the signal processing are gathered in Table 1, where τ and Q_{tot} express respectively the time to reach the maximum value of heat flow rate and the total heat quantity released from the dissolution reaction. As noted in Table 1, one can notice that Q_{tot} and τ increase with the phosphate mass. The total heat flow was measured by integrating the curve of the heat quantity as a function of time.

Here Table 1.

Fig. 3 shows that the variation of the heat quantity released during the dissolution is linearly proportional to the phosphate mass. The total heat quantity per unit of mass, i.e., dissolution enthalpy, is equal to -229.1 J g^{-1}.

Here Fig. 3

The previous experiments were repeated by using the mixture solution S2 and by varying the mass. The evolution of heat flow rate with time versus phosphate mass is represented in Fig. 4.

Here Fig. 4

For the case of the phosphate PG1 dissolution in the mixture solution of phosphoric and sulfuric acids, one can notice the presence of two peaks which are more pronounced when the phosphate mass decreases. The time to reach the maximum heat flow rate of the first peak remains almost constant. On the other side, the second peak came closer to the first and overlap by increasing the mass. Antar and Jemal [10] confirmed this phenomenon from their analyses. By using X-Ray Diffraction method (XRD), they showed that the first peak corresponds to the phosphate dissolution by phosphoric acid and the formation of HH precipitation, the second peak corresponds to the transformation of the HH precipitate to DH precipitate by sulfuric acid.

The plot of the total heat amount versus sample mass gave a linear curve as shown in Fig. 5, with a slope equal to -301 J g^{-1}. In fact, it is remarkable that the heat released per amount of phosphate in the solution of the mixed acids S2 is higher than that the one done with only phosphoric acid solution S1, which was equal to -229.1 J g^{-1}. This is due to the precipitation of calcium sulfate in the presence of sulfuric acid.

Here Fig. 5

To study the kinetics of the natural rock dissolution containing various impurities, Avrami (1941) model [15] was used to interpret the results of the calcium sulfate precipitation in S2 solution [16-17]. The general form of this model is written as:

$$-\ln(1-x) = kt^n \tag{7}$$

where, k and n are the Avrami constants. The term x is the ratio between the heat amount released at time t and the total heat amount released. To apply this model, a curve which express ln(-ln(1-x)) was plotted as a function of ln(t). Fig. 6 shows the Avrami curves of phosphate (PG1) dissolution in S2.

Here Fig. 6

As it is shown in Fig. 6, for each curve there are three fields, which were identified as:

- Field I: dissolution of phosphate by phosphoric acid,
- Field II: formation of the precipitate hemihydrate,
- Field III: transformation of the precipitate hemihydrate to the precipitate dihydrate.

The calculation of the slope and the intercept of each line, which represents only one field, determines the constants of Avrami k and n (Table 2). As mentioned earlier, Table 2 shows that the time to reach the first peak is almost constant, while the time for the second decreases by increasing the mass. The constants of Avrami k and n are nearly constant for the four experiments, which means that the same phenomenon was repeated at each experiment of dissolution.

Here Table 2.

3.2. Dissolution of low phosphate from Cheketma-Kasserine (PK1) in acid solutions at 25°C

This section focuses on the dissolution of the natural low phosphate of Cheketma-Kasserine (PK1) in acid solutions S1 and S2. The dissolution of the rock in S1 gave the calorimetric signals displayed in Fig. 7, with the same shape as for the dissolution of PG1 in S1 (Fig. 1).

Here Fig. 7

Figure 8 shows the linear relationships between the total heat released and the phosphate mass in the solution S1. The total dissolution heat per unit of mass is equal to -225.3 J g^{-1}.

Here Fig. 8

For the dissolution of the sample PK1 in the solution S2, the evolution of the heat flow rate is displayed in Fig. 9. The total dissolution heat per unit of mass is equal to -342.3 J g^{-1} (Fig. 10). One can notice the absence of a second peak for the dissolution of the phosphate PK1. This is due to the low concentration of P_2O_5 making the second exothermic reaction not detectable.

Here Fig. 9

Here Table 3

Here Fig. 10

Table 3 exposes the total heat amount of each dissolution experiment and the Avrami constants that are nearly equal, which means that the same phenomenon was repeated at each experiment of dissolution. Compared to the Gafsa phosphates (PG1), only two domains were identified by using Avrami method. This is due to the fact that the second step is not detectable by this calorimetric method.

3.3. Influence of granulometry on dissolution of phosphates.

One can notice that the heat quantity of the total dissolution of PG1 is similar to that of PK1 in both solution S1 and S2. This similarity is strange because P_2O_5 concentration in sample PK1 is lower than in sample PG1. This observation might be due to a mass and heat transfer resistant due to the particle size distribution.

To verify the role of granulometry, a third sample was used which is the PK2 obtained by crushing the sample PK1. The calorimetric signals of dissolution in the solution S1 with various masses are displayed in Fig. 11. The total heat amount per unit of mass, for the dissolution of PK2 in S1 is equal to -247.6 J g^{-1}.

Here Fig. 11

Here Fig. 12

The evolution of heat flow rate for the dissolution of PK2 in the solution S2 is shown in Fig. 13. The plot of the heat quantity as function of the dissolved mass is displayed in Fig. 14, where the total heat per unit of the dissolved phosphate mass is equal to -397.8 J g^{-1}.

Here Fig. 13

Here Fig. 14

Table 4 summarizes the heat flow released during the dissolution of PG1, PK1 and PK2 in S1 and S2.

Here Table 4

From Table 4, one can notice that granulometry plays an important role on the kinetics of dissolution. Thus, kinetics of dissolution by using smaller granulometry will be faster, but will release more heat which could lead to a thermal runway.

4. Conclusion

The dissolution of natural phosphate rocks by different mineral acids was studied in this manuscript by using micro-calorimetry. The goal was to study the dissolution of Cheketma-Kasserine natural phosphate rocks and to compare with the dissolution of natural phosphate rocks from Gafsa region, whose concentration in phosphorous pentoxyde is higher.

It was observed that by using a similar granulometry distribution, i.e., lower than 500 µm, the specific heat released by the dissolution of both natural rocks by phosphoric acid solution was the same, i.e., -230 J g^{-1}.

The dissolution of Gafsa phosphate by using a mixed mineral acid solution (phosphoric and sulfuric acid) presented a different thermal behavior. Indeed, two different peaks appeared on the thermogram due to the second reaction of calcium sulfate precipitation. Specific heat was similar for the dissolution of both phosphate samples and was comprised between -300 and -350 J g^{-1}. This energy was higher than in the case of phosphoric acid dissolution due to the second reaction. By using the Avrami model, three domains were observed for Gafsa phosphate and two for Cheketma-Kasserine phosphate.

A different granulometry distribution was used for the Cheketma-Kasserine phosphate, i.e., lower than 120 µm. It was observed that the specific heat released during the dissolution by phosphoric acid solution or by the mixed mineral acid solution was higher than with a granulometry distribution lower than 500 µm. This information is essential to design a proper heat transfer system.

Figures

Fig. 1 Schematic view of the C80 cells.

Fig. 2 Dissolution of the enriched phosphate PG1 in the solution S1 at 25°C at different sample mass.

Fig. 3 The amount of heat dissolution of the enriched phosphate PG1 in the solution S1 according to the sample mass.

Fig. 4 Dissolution of the enriched phosphate PG1 in the solution S2 at 25°C at different sample mass.

Fig. 5 The amount of heat dissolution of the enriched phosphate PG1 in the solution S2 in function of sample mass.

Fig. 6 $\ln(-\ln(1-x))=f(\ln(t))$ during the dissolution of the phosphate attack by the solution S2 at 25°C according to the mass (a : 50.07 mg, b : 101.59 mg, c : 201.60 mg, d : 300.92 mg).

Fig. 7 Dissolution of the low phosphate PK1 in the solution S1 at 25°C at different sample mass.

Fig. 8 The amount of heat dissolution of the low phosphate PK1 in the solution S1 according to the sample mass.

Fig. 9 Dissolution of the various weights of the low phosphate PK1 in the solution S2 at 25°C.

Fig. 10 The amount of heat dissolution of the low phosphate PK1 in the solution S2 according to the sample mass.

Fig. 11 Thermogram of phosphate PK2 dissolution in solution S1 at 25°C.

Fig. 12 The amount of heat dissolution of the low phosphate PK2 in the solution S1 according to the sample mass.

Fig. 13 Dissolution of the various weights of the low phosphate PK2 in the solution S2 at 25°C.

Fig. 14 The amount of heat dissolution of the low phosphate PK2 in the solution S2 according to the sample mass.

Fig. 15 Dissolution of 260.99 mg of PG2 in the solution S2 at 25°C.

Tables

Acknowledgments

The authors gratefully acknowledge the support of this work to the research Unit of Applied Thermodynamics and at the National School of Engineers of Gabes and the *Laboratoire de Sécurité des Procédés Chimiques (LSPC)* at INSA Rouen.

References

1. Mohammadkhani M, Noaparast M, Shafaei SZ, Amini A, Amini E, Abdollahi H. Double reverse flotation of a very low grade sedimentary phosphate rock, rich in carbonate and silicate. International Journal of Mineral Processing. 2011;100:157–65.

2. Gharabaghi M, Noaparast M, Irannajad M. Selective leaching kinetics of low-grade calcareous phosphate ore in acetic acid. Hydrometallurgy. 2009;95:341–5.

3. Amorri, Z. Réduction de la teneur en matière organique contenue dans l'acide phosphorique de voie humide par le peroxyde d'hydrogène et l'argile naturelle. PhD dissertation, National Engineering School of Gabes, Tunisia, 2012.

4. Pereira, F. Production d'acide phosphorique par attaque chlorhydrique de minerais phosphatés avec réductions des nuisances environnementales et récupération des terres rares entant que sous-produits. PhD dissertation, Ecole Nationale Supérieure des Mines de Saint-Etienne, France, 2003.

5. Sikdar, S.K., Ore, F., Moore, J.H. Crystallisation of calcium sulfate hemihydrate in reagent-grade phosphoric acid. AIChE Symposium Series. 1980 ;76(193):82-9.

6. Antar K, Brahim K, Jemal M. Étude cinétique et thermodynamique de l'attaque d'une fluorapatite par des mélanges d'acides sulfurique et phosphorique À 25°C. Thermochim Acta. 2006;449:35–41.

7. Brahim K, Khattech I, Dubès JP, Jemal M. Etude cinétique et thermodynamique de la dissolution de la fluorapatite dans l'acide phosphorique. Thermochim Acta. 2005;436:43–50.

8. Van der Sluis S, Meszaros Y, Marchee WGJ, Wesselingh HA, Van Rosmalen GM. The digestion of phosphate ore in phosphoric acid. Ind Eng Chem Res. 1987;26:2501–5.

9. Brahim K, Antar K, Khattech I, Jemal, M. Effect of temperature on the attack of fluorapatite by a phosphoric acid solution. Sci Res Essay. 2008;3(1),35–9.

10. Antar K, Jemal M. Kinetics and thermodynamics of the attack of a phosphate ore by acid solutions at different temperatures. Thermochim Acta. 2008;474:32–5.

11. Vaimakis TC, Economou ED, Trapalis CC. Calorimetric study of dissolution kinetics of phosphorite in diluted acetic acid. J Therm Anal Calorim. 2008;92:783–9.

12. Soussi-Baatout A, Hichri M, Bechrifa A, Khattech I. Test and calibration processes for the differential reaction calorimeter (DRC): Application: Dissolution of calcium fluorapatite in the hydrochloric acid. Thermochim Acta. 2014;580:85–92.

13. Zheng JL, Wärnå J, Salmi T, Burel F, Taouk B, Leveneur S. Kinetic modeling strategy for an exothermic multiphase reactor system: Application to vegetable oils epoxidation using Prileschajew method. AIChE J. 2016;62:726–41.

14. Rakotondramaro H, Wärnå J, Estel L, Salmi T, Leveneur S. Cooling and stirring failure for semi-batch reactor: Application to exothermic reactions in multiphase reactor. J Loss Prev Process Ind. 2016;43:147–57.

15. Avrami M. Granulation, phase change, and microstructure kinetics of phase change. III. The Journal of Chemical Physics. 1941;9:177–84.

16. Okur H, Tekin T, Ozer A.K, Bayramoglu M. Effect of ultrasound on the dissolution of colemanite in H_2SO_4. Hydrometallurgy. 2002;67:79–86.

17. Sevim F, Saraç H, Kocakerim MM, Yartaşı A. Dissolution kinetics of phosphate ore in H_2SO_4 Solutions. Ind Eng Chem Res. 2003;42:2052–7.

Figure

Figures

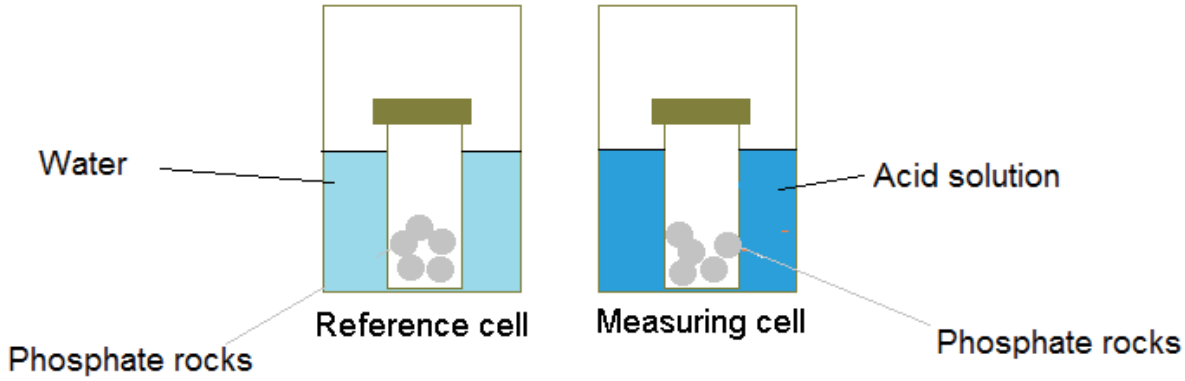

Fig.1 Schematic view of the C80 cells.

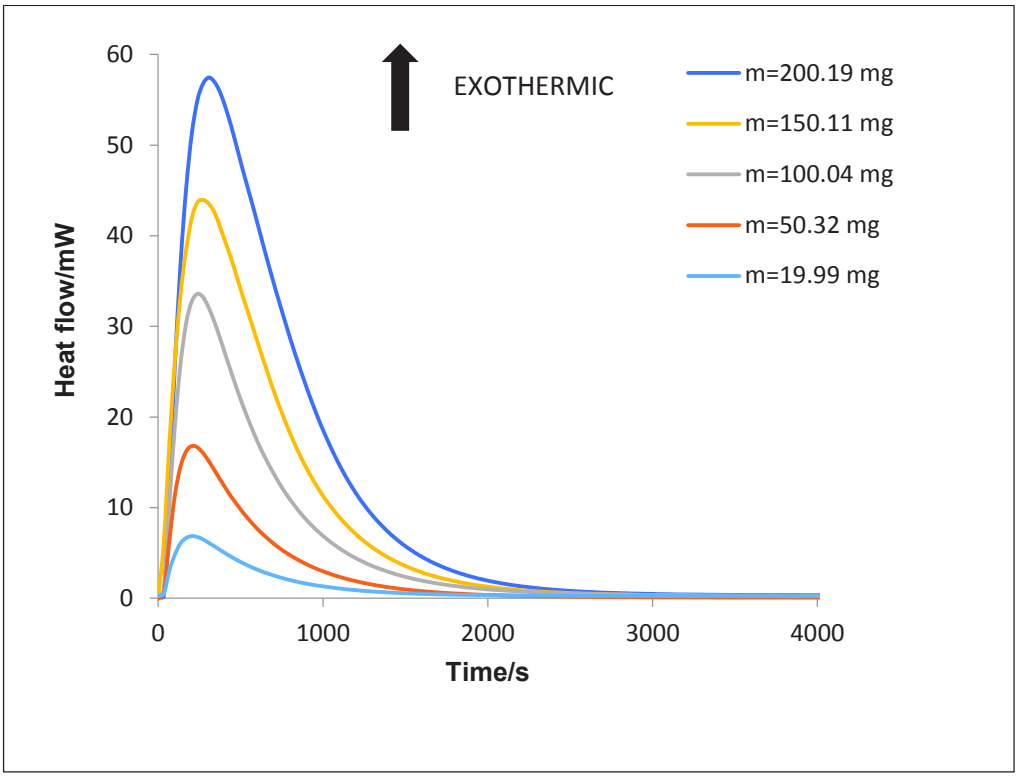

Fig.2. Dissolution of the enriched phosphate PG1 in the solution S1 at 25°C at different sample mass.

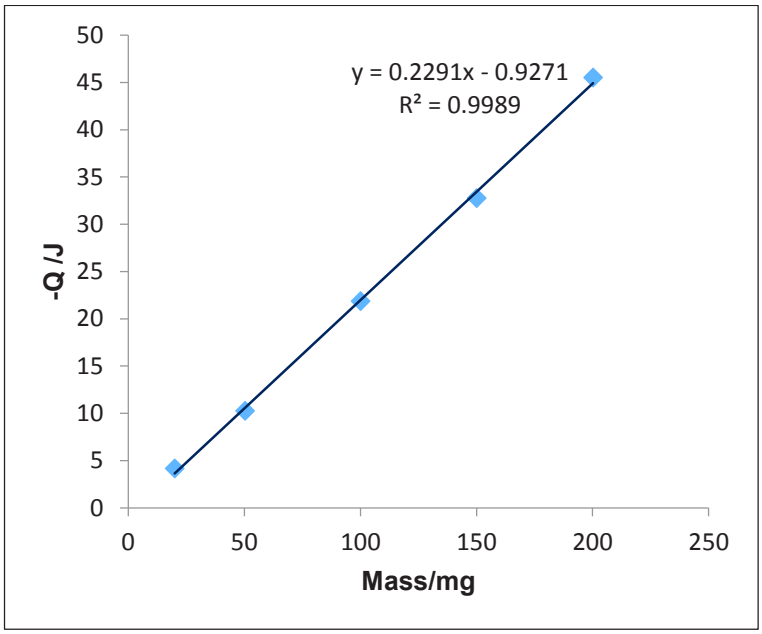

Fig.3 The amount of heat dissolution of the enriched phosphate PG1 in the solution S1 according to the sample mass.

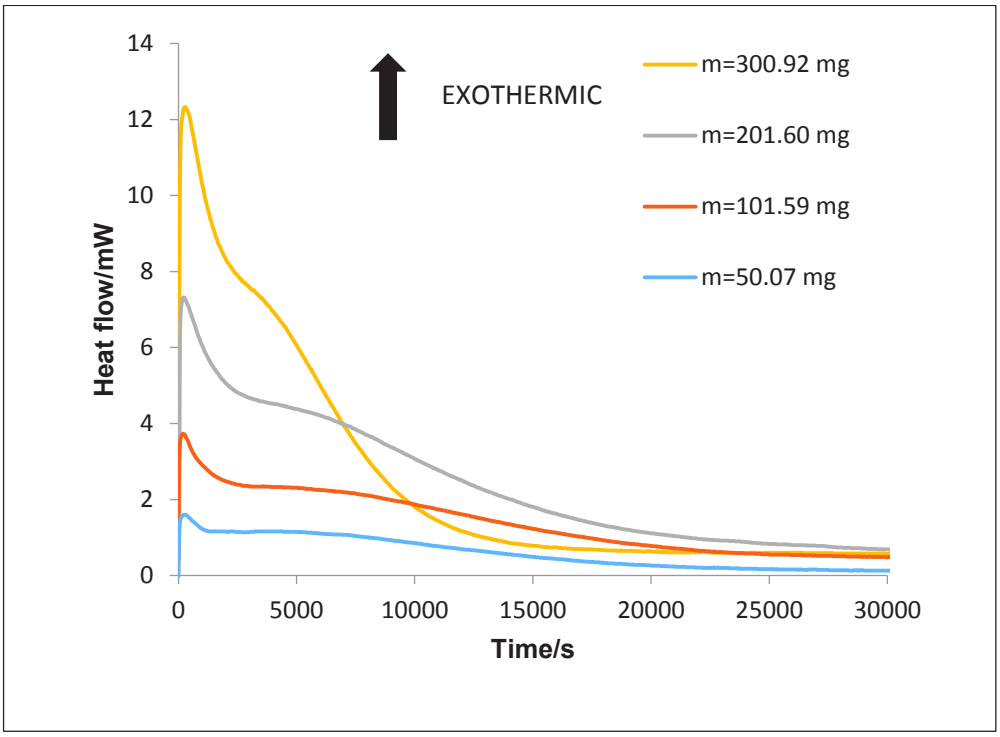

Fig.4 Dissolution of the enriched phosphate PG1 in the solution S2 at 25°C at different sample mass.

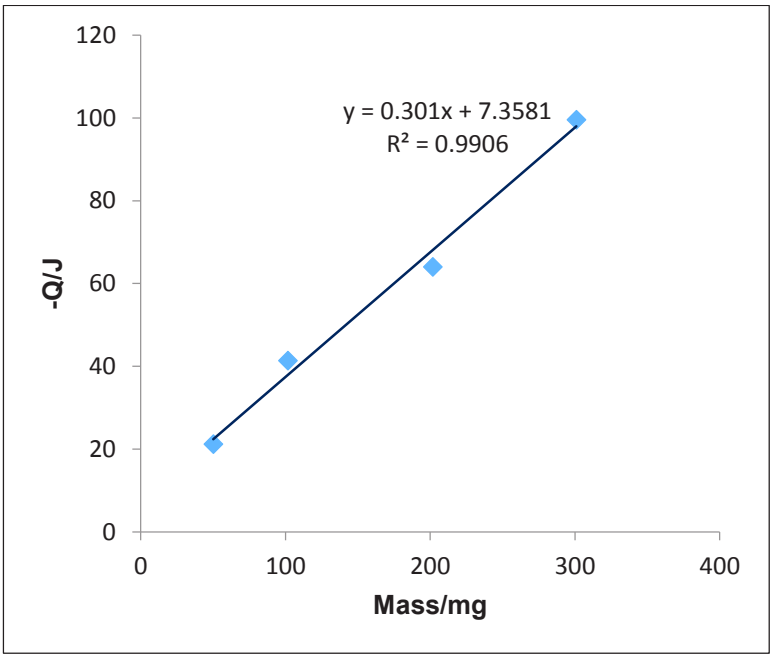

Fig.5 The amount of heat dissolution of the enriched phosphate PG1 in the solution S2 in function of sample mass.

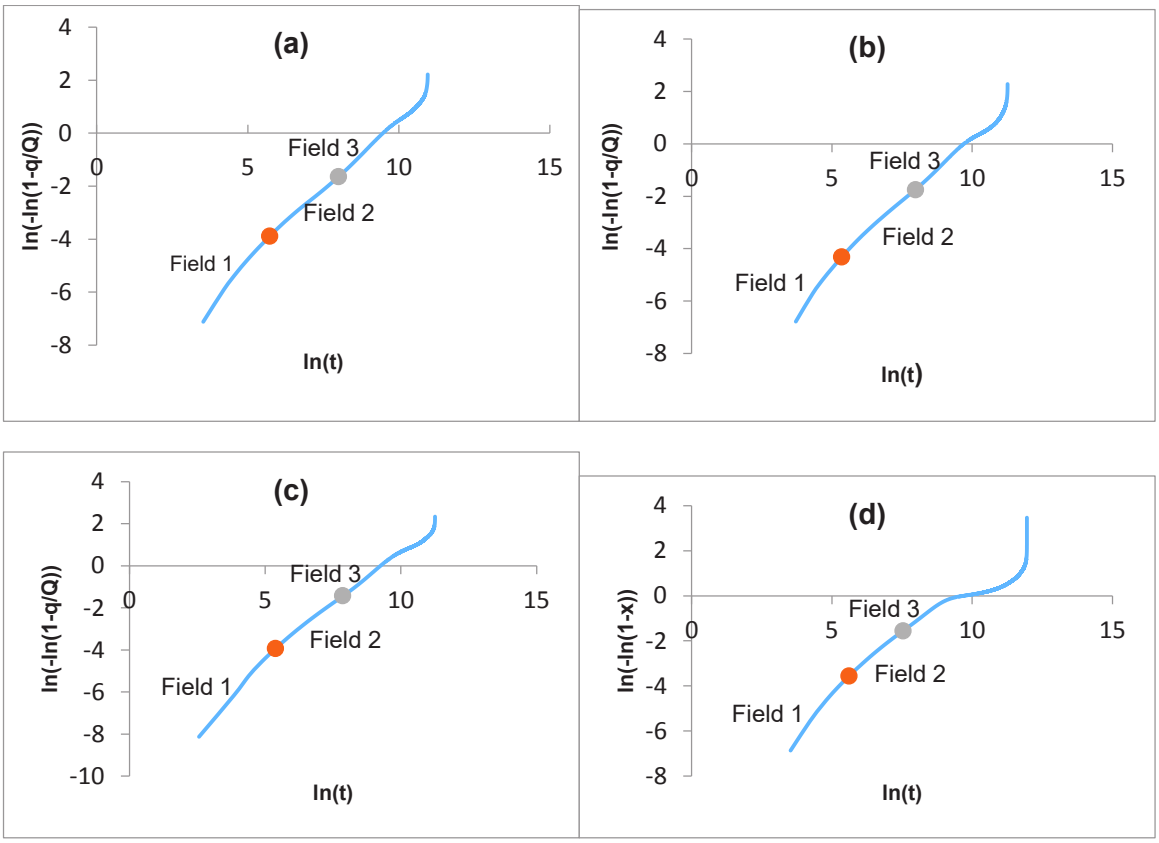

Fig.6 ln(-ln(1-x))=f(ln(t)) during the dissolution of the phosphate attack by the solution S2 at 25°C according to the mass (a : 50.07 mg, b : 101.59 mg, c : 201.60 mg, d : 300.92 mg).

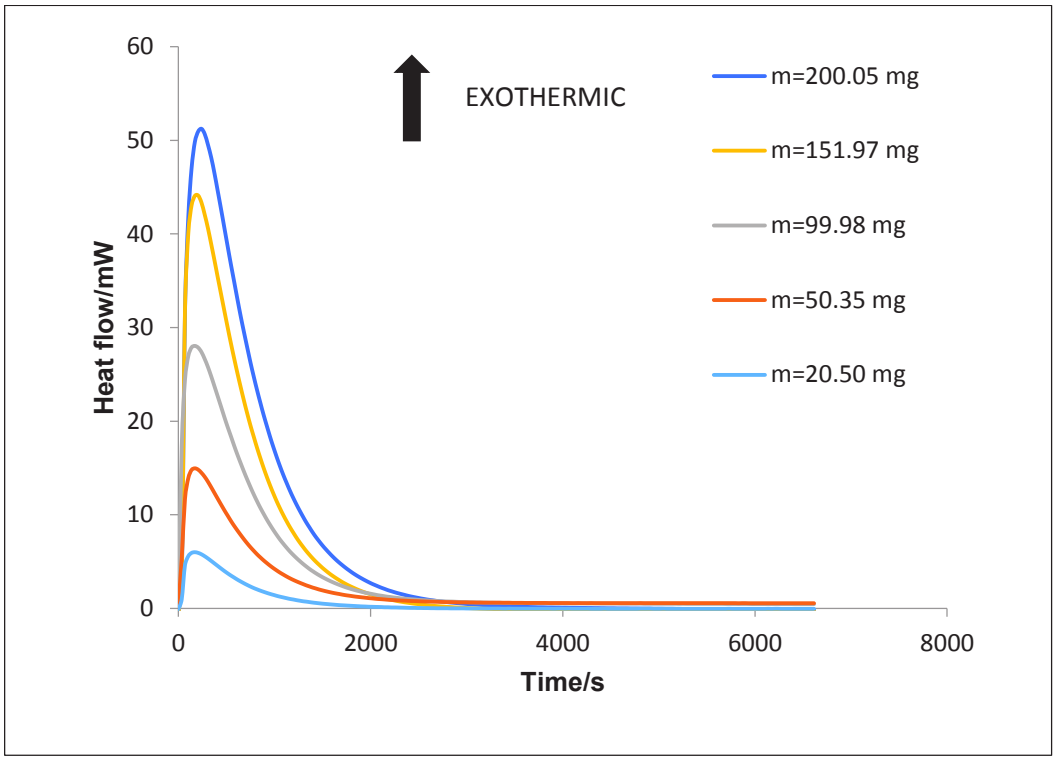

Fig.7 Dissolution of the low phosphate PK1 in the solution S1 at 25°C at different sample mass.

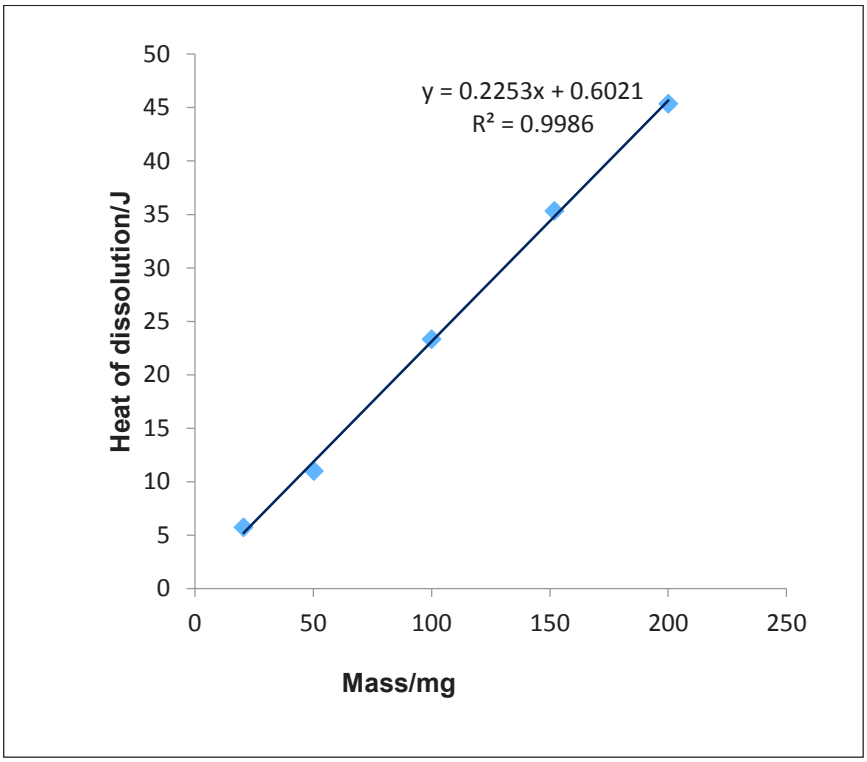

Fig.8 The amount of heat dissolution of the low phosphate PK1 in the solution S1 according to the sample mass.

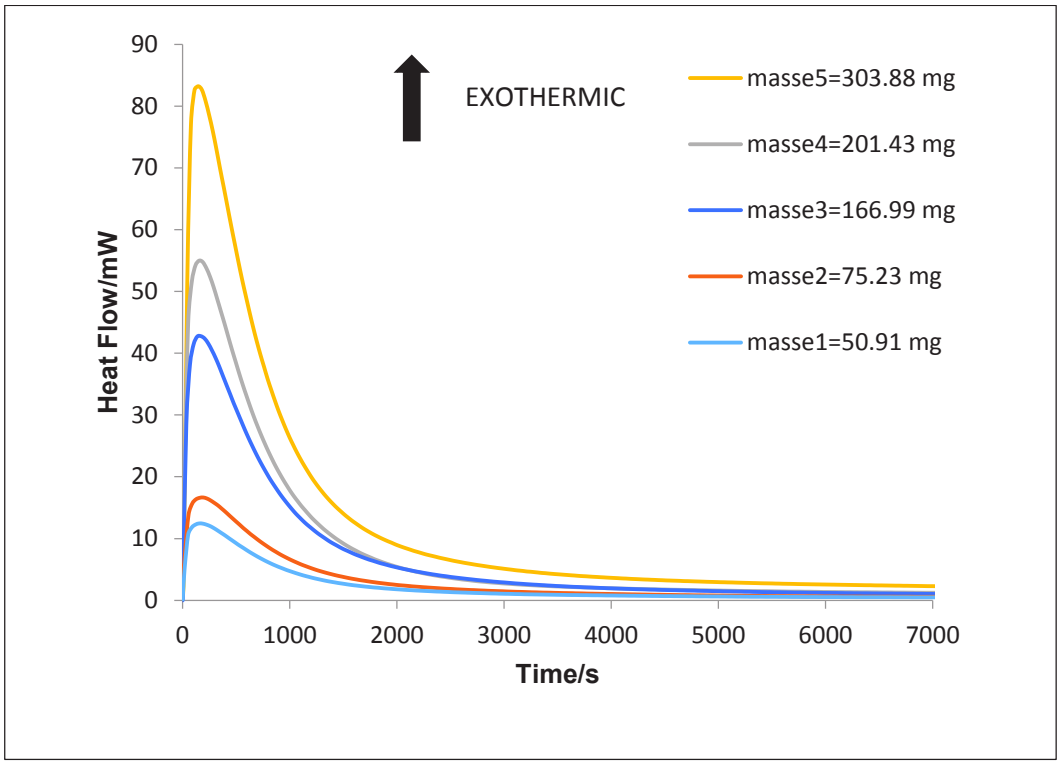

Fig.9 Dissolution of the various weights of the low phosphate PK1 in the solution S2 at 25°C.

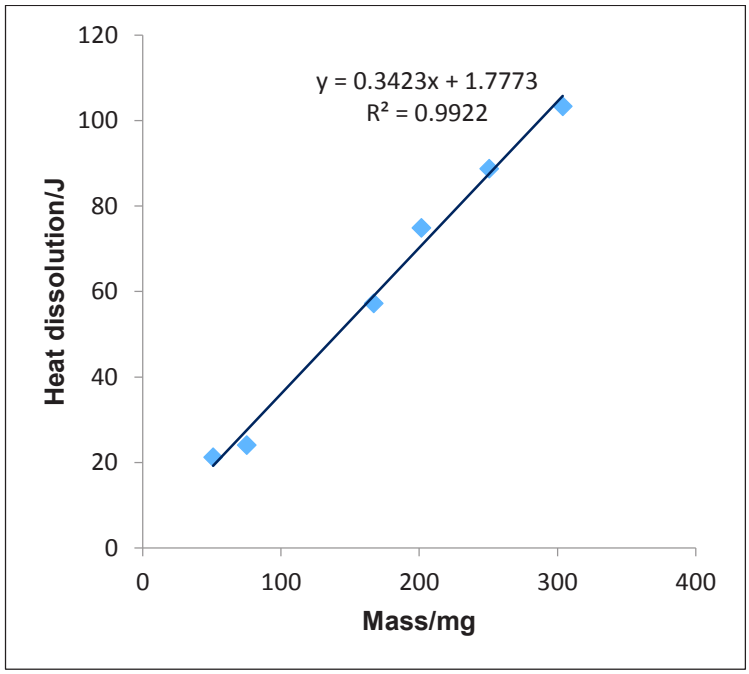

Fig.10 The amount of heat dissolution of the low phosphate PK1 in the solution S2 according to the sample mass.

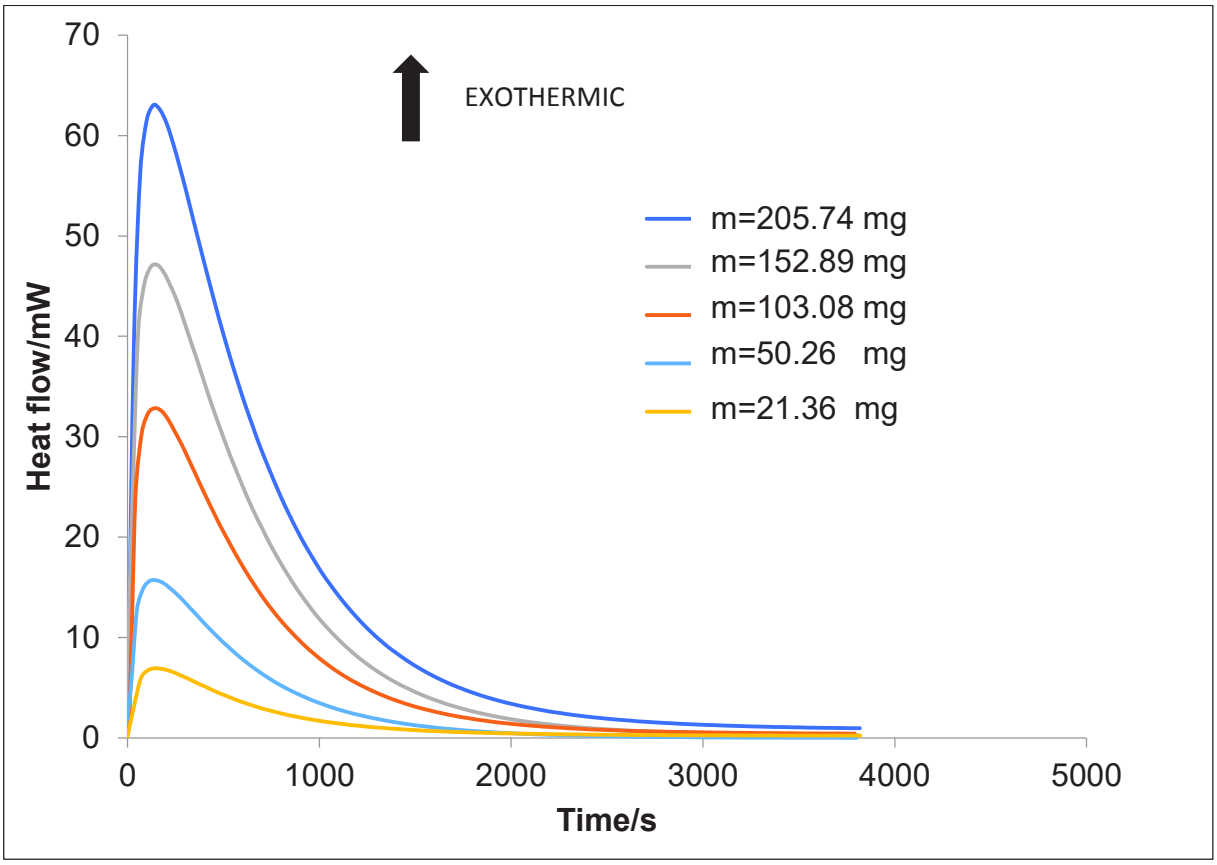

Fig.11 Thermogram of phosphate PK2 dissolution in solution S1 at 25°C.

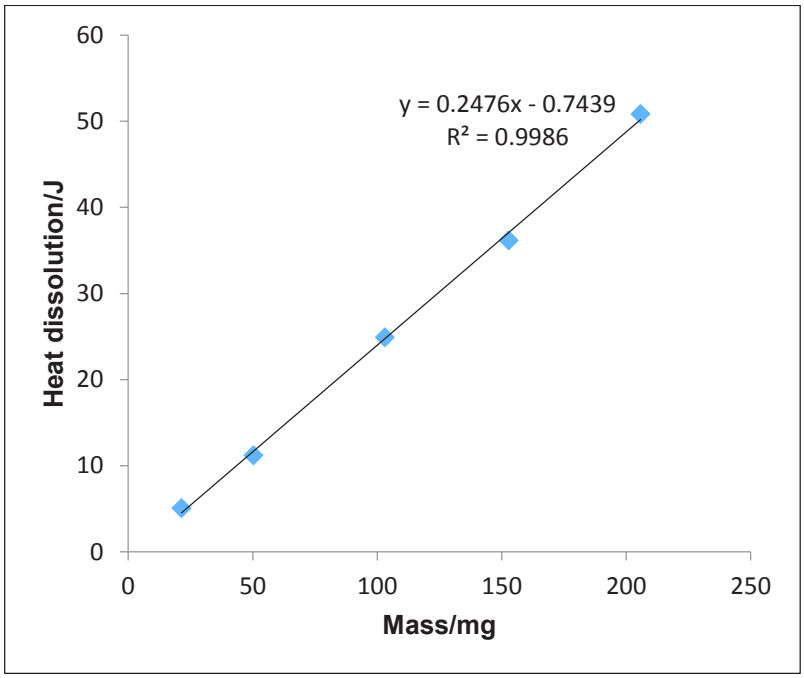

Fig.12 The amount of heat dissolution of the low phosphate PK2 in the solution S1 according to the sample mass.

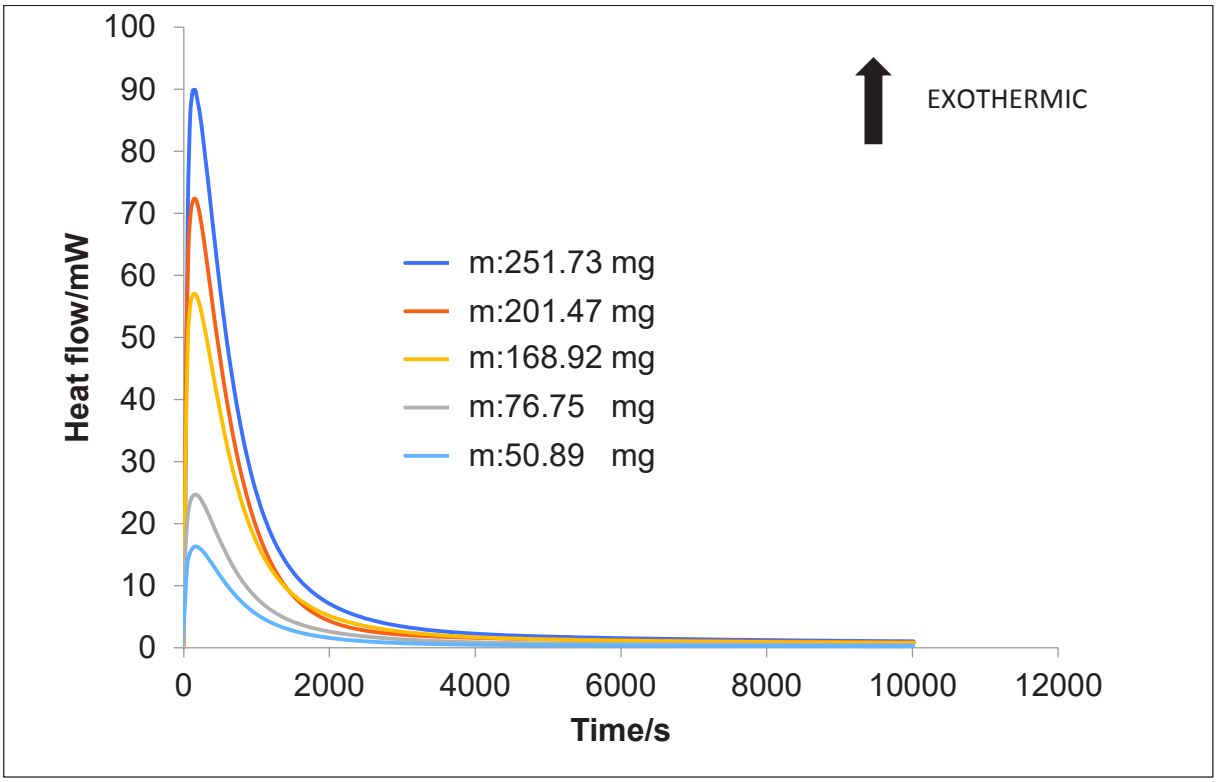

Fig.13 Dissolution of the various weights of the low phosphate PK2 in the solution S2 at 25°C.

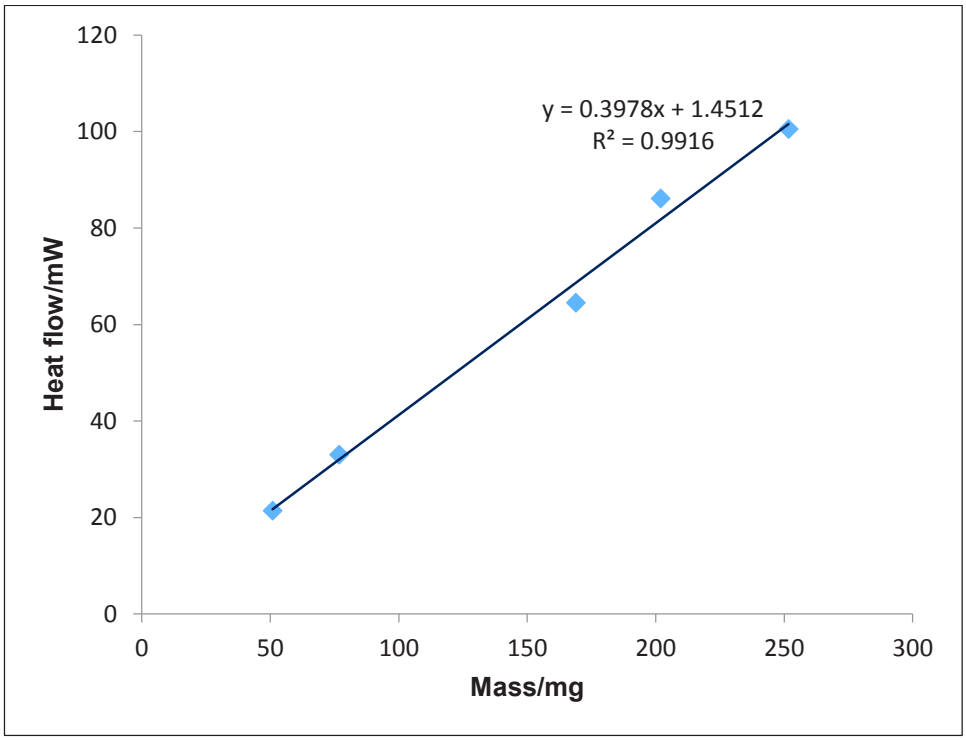

Fig.14 The amount of heat dissolution of the low phosphate PK2 in the solution S2 according to the sample mass.

Tables

Table 1 Calorimetric data for the dissolution of PG1 in solution S1.

Mass/g	**τ/s**	**Q_{tot}/J**
19.99	204	-4.18
50.32	205	-10.27
100.04	238	-21.88
150.11	273	-32.76
200.19	307	-45.53

Table 2 Avrami constants calculated for the dissolution of PG1 in S2.

Mass/mg	50.07	101.59	201.60	300.92
Time at the end of the Field 1/s	307	212	218	273
Time at the end of the Field 2/s	3001	2933	2592	1876
k1 of Field 1	$5.792\ 10^{-6}$	$4.799\ 10^{-6}$	$6.511\ 10^{-6}$	$4.680\ 10^{-5}$
n1 of Field 1	1.443	1.494	1.503	1.571
k2 of Filed 2	$9.271\ 10^{-5}$	$9.823\ 10^{-5}$	$11.20\ 10^{-5}$	$9.930\ 10^{-5}$
n2 of Field 2	0.953	0.941	0.977	1.020
k3 of Filed 3	$2.068\ 10^{-5}$	$4.742\ 10^{-5}$	$5.325\ 10^{-5}$	$16.67\ 10^{-5}$
n3 of Field 3	1.138	1.027	1.062	0.947

Table 3 Avrami constants calculated for the dissolution of PK1 in S2.

Mass/mg	50.91	75.23	166.99	201.43	303.88
Time at the end of the Field 1/s	153	191	171	153	145
k1 of the Field 1	$6.911\ 10^{-5}$	$6.99\ 10^{-5}$	$3.14\ 10^{-5}$	$9.16\ 10^{-5}$	$5.115\ 10^{-5}$
n1 of the Field 1	1.35	1.399	1.611	1.36	1.98
k2 of the Field 2	$32.51\ 10^{-5}$	$31.37\ 10^{-5}$	$35.31\ 10^{-5}$	$30.77\ 10^{-5}$	$26.66\ 10^{-5}$
n2 of the Field 2	1.054	1.114	1.138	1.131	1.167

Table 4 Heat dissolution of the phosphate PG1, PK1 and PK2 in S1 and S2.

	Phosphate PG1	Phosphate PK1	Phosphate PK2
Heat dissolution of phosphates in the solution S1/J g^{-1}	-229.1	-225.3	-247.6
Heat dissolution of phosphates in the solution S2/J g^{-1}	-301.0	-342.3	-397.8